

## Bio-sorption of methylene blue using *Datura stramonium* leaves as adsorbent

**Maty Mossane Diouf**

Department of Chemistry, Faculty of Sciences and Technology, University Cheikh Anta Diop, Dakar, 10700, Senegal

**Ramatoulaye Diouf**

Department of Chemistry, Faculty of Sciences and Technology, University Cheikh Anta Diop, Dakar, 10700, Senegal

**Aïssatou Alioune Gaye\***

Department of Chemistry, Faculty of Sciences and Technology, University Cheikh Anta Diop, Dakar, 10700, Senegal  
e-mail: aissatoualioune1ster@gmail.com

**Alioune Fall**

Department of Chemistry, Faculty of Sciences and Technology, University Cheikh Anta Diop, Dakar, 10700, Senegal

### Abstract

Present study was accomplished to prospect the viability of using the *Datura stramonium* leaves powder (DS) as an adsorbent to remove the methylene blue from aqueous solution. The physico-chemical characteristics of the studied adsorbent were examined. The optimum parameters such as contact time, particle size, adsorbent dose, initial methylene blue concentration, and pH were investigated by performing batch experiments models. The kinetics and the isotherms adsorption were evaluated by varying the initial concentration and using the optimum parameters. The optimum of contact time is 30min, with a removal capacity of 89.60 %. The optimal adsorbent concentration to reach the maximum removal of methylene blue (89.54 %) is 18 g/L. An initial methylene blue concentration of 50 ppm is ideal to reach the maximum capacity of removal (92.72 %). The optimum particle size is 80  $\mu\text{m}$ . The kinetics of the adsorption process are in accordance with the pseudo-second order model. Experimental values of the adsorption capacity are close proximity to the optimum values predicted by the pseudo-second order model. Langmuir, Freundlich, Temkin, Dubinin-Radushkevich, Harkin-Jura and Hasley isotherms were applied to represent the data obtained from the adsorption studies. The highest  $R^2$  values were related to Freundlich, Dubinin-Radushkevich and Hasley isotherm models.

### 1. Introduction

Textile is a sector that contributes significantly to the resources of many countries. Despite its importance in the economy, it induces very significant environmental impacts [1–4]. The textile industry is partly responsible for water pollution by discharging large quantities of dyes that are often accompanied by various organic and mineral pollutants. Various dyes such as methylene blue, Eriochrome black T, indigo red, carmine, rhodamine, and red 120 are widely used in the textile industry [5–8]. It is one of the most polluting industries. Consequently, the sanitation of industrial wastewater is a major issue to avoid large-scale pollution of water resources used by populations for their drinking water supply. Indeed, these pollutants, which are often recalcitrant, induce negative consequences that can lead to irreversible effects on human and animal health [9–

Received: October 2, 2024; Accepted: November 1, 2024; Published: November 5, 2024

Keywords and phrases: dye, isotherm, kinetic, adsorption, methylene blue, *Datura stramonium*.

12]. Weeping expensive strategies such as the advanced oxidation process, membrane processes, adsorption on specific surfaces and numerous physical process, are developed and put into service in several industries in order to reduce the pollutant load before discharging wastewater into nature [13–17]. The implementation in the industry of wastewater treatment by the method of adsorption on activated carbon has led to the search for a less expensive and simpler alternative to implement [18–21]. The recovery of waste from the use of biomass, the disposal of which is expensive, has made it possible to develop other types of effective and very low-cost adsorbents [22–24].

Within this context, we selected *Datura stramonium* leaves (DS) to remove methylene blue (MB) from wastewater. Optimal adsorption parameters were determined before examination isotherms and kinetics models of the adsorption of methylene blue on leave powder of *Datura stramonium*.

## 2. Material and Methods

### 2.1. Preparation of the adsorbent

*Datura stramonium* was harvested at Mbetit Gouye (Fatick Region in Senegal 14°25'59.99''N, 16°31'59.99''O). The leaves (DS) were collected and rinsed twice with tap water first and distilled water to remove all the particles. They were shadow dried for three days. After this first process, the DS were dried at 50°C for 48 hours. The DS were ground using a grinder. This EHL were stored in a plastic container. The dried DS adsorbent was again crushed and sieved to get different sized fractions, namely, 80, 100, 125, 250, 315, 400, 500, 1500  $\mu\text{m}$ . These different fractions were stored in airtight containers for further use.

### 2.2. Point zero charge $\text{pH}_{\text{PZC}}$

The pH of the point of zero charge ( $\text{pH}_{\text{PZC}}$ ) for the *Datura stramonium* leaves (DS) was determined by a titration procedure. To a series of eleven 150 mL conical flasks 45 mL of a solution of  $\text{KNO}_3$  0.01 M were added and the pH was accurately adjusted using HCl or NaOH 0.01 N solutions from pH = 2 to pH = 12 and completed with a solution  $\text{KNO}_3$  0.01 M to 50 mL. The initial pH ( $\text{pH}_i$ ) was accurately measured again. To each flask, 0.1 g of DS was added, and the flask was capped and shaken manually each 4 hours. After 48 hours, the final pH ( $\text{pH}_f$ ) was measured. The  $\Delta\text{pH} = \text{pH}_f - \text{pH}_i$  is plotted against  $\text{pH}_i$ . The point of intersection of the curve and the abscissa axe at  $\Delta\text{pH} = 0$  gave the  $\text{pH}_{\text{PZC}}$ .

### 2.3. Batch adsorption tests

All the experiments were conducted in discontinuous batch. A weighed sample of DS was mixed with 50 mL of the methylene blue (scheme 1) solution in 150 mL conical flasks. The mixture was stirred for a fixed time at 25°C. After this process, the liquid was separated from the adsorbent by filtration through a Whatman Filter N°1. The residual methylene blue concentration was determined using a Lambda 365 UV/Vis Perkin-Elmer spectrophotometer. The experimental data were used to determine the removal capacity, and the quantity of methylene blue adsorbed on the DS:

$$\text{Removal capacity} = \frac{(C_0 - C_e) \times V}{C_0} \times 100$$

$$q_e = \frac{(C_0 - C_e) \times V}{m}$$

where  $C_0$  and  $C_e$  are respectively the initial and the final metal concentrations (mg/L) in the liquid phase,  $V$  (L) is the volume of the liquid phase and  $m$  (g) is the adsorbent mass used.

#### 2.4. Effect of time contact on the removal capacity

The equilibrium time was determined using a Methylene Blue solution at a concentration of 50 ppm. Each 50 mL Methylene Blue solution was treated with 0.25 g of DS at time ranging from 10 to 180 minutes. The experiments were conducted at the same pH and the flasks contents were stirred at 500 rpm at a temperature of 25°C.

#### 2.5. Adsorbent dose effect on the removal capacity

50 mL of a 50 ppm methylene blue solution was treated with a mass of adsorbent ranging from 0.1 to 1.0 g. The experiments were conducted at the same pH and the flasks contents were shaken at 500 rpm at temperature of 25°C for the optimal time determined previously.

#### 2.6. Effect of adsorbent particle size on the removal capacity

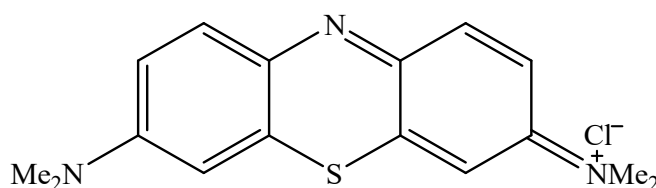
The ideal particle size for the adsorbent was determined by treating each category (80,100, 125, 250, 315, 400, 500 and 1500  $\mu\text{m}$ ) with 50 mL of a 50 ppm Methylene Blue solution at the optimum pH using 0.9 g of DS powder. The flasks were shaken at 500 rpm and at a temperature of 25°C for the optimal time determined previously.

#### 2.7. Effect of solution pH on the removal capacity

The effect of solution pH on the dyes removal capacities of the adsorbent was investigated between  $\text{pH} = 2$  and  $\text{pH} = 11$ . The experiments were performed by adding a 0.9 g of DS powder (particle size 80  $\mu\text{m}$ ) into six 150 mL conical flasks containing 50 mL of 50 ppm dye solutions and the pH of the solution was adjusted using 0.1 N HCl or 0.1 N NaOH. The flasks were shaken at 500 rpm and at temperature of 25°C for the optimal time determined previously.

#### 2.8. Effect of methylene blue solution concentration on the removal capacity

The effect of dye solution on the removal capacity were determined by setting the optimum temperature, granulometry of the adsorbent, the pH of the solution and adsorbent dose and varying the methylene blue concentration between 10 to 100 ppm. The flasks contents were stirred at 500 rpm at a temperature of 25°C for the optimal time determined previously.



**Scheme 1.** Structural formulae of methylene blue.

### 3. Results and Discussion

#### 3.1. Infrared spectra

The FTIR spectrum of powder leaves of *Datura stramonium* (DSL) and FTIR spectrum of powder leaves of *Datura stramonium* after treatment of aqueous blue methylene solution (DSL-MB) were recorded on the Perkin Elmer spectrophotometer Two in the range 4000 – 400  $\text{cm}^{-1}$ . In both spectra, the broad bands pointed at approximately 3290  $\text{cm}^{-1}$  are characteristic of associated –OH groups which is present in phenolic and carboxylic acid [25]. Bands present in the range 2980–2800  $\text{cm}^{-1}$  are due to the stretching and bending modes of the –CH of the methylene and the methyl groups. The intense bands at 1634  $\text{cm}^{-1}$  are attributed to the C=O groups. The bands located in the range 1580–1400  $\text{cm}^{-1}$  are attributed to the C=C in aromatic rings. Multiple vibrations due to the C–O moiety are pointed in the region 1230–1000  $\text{cm}^{-1}$ . The sorption of methylene blue is attested by the change of the intensity of the vibrational frequency of functional groups within the range 4000–400 $\text{cm}^{-1}$  before and after adsorption of methylene blue.

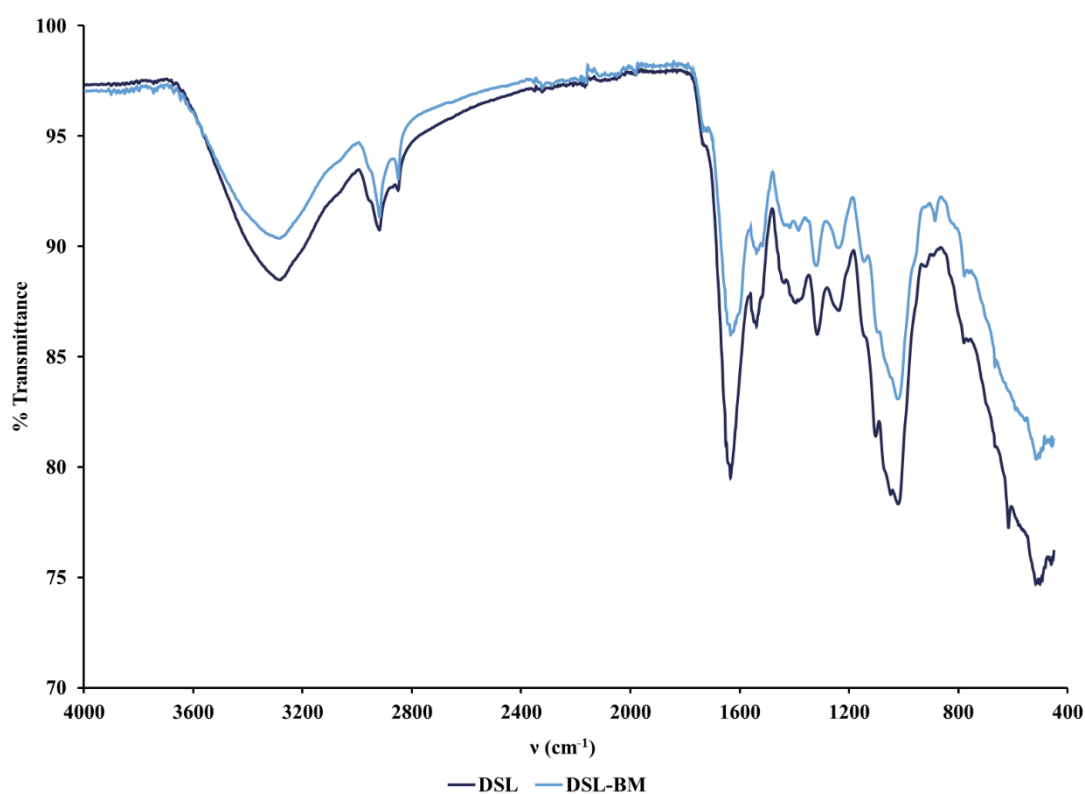


**Figure 1.** FTIR spectrum of DSL and DSL-MB.

#### 3.2. Optimization of methylene blue removal the parameters

To determine the best conditions for adsorption of methylene blue using *Datura stramonium* leaves (DSL) as adsorbent, certain parameters such as contact time, amount of adsorbent used, particle size, pH or initial concentration of the blue methylene solution were studied.

The adsorption capacity of *Datura stramonium* leaves is studied as a function of contact time because of the role that the latter can play on the adsorption equilibrium (Figure 2). We work with an adsorbate solution of 50 mg/L initially. After 10 minutes, we observed an adsorption rate of 86.55%. The adsorption rate continues to

increase very slowly and reaches a maximum of 89.60% after 30 minutes. Subsequently, the adsorption rate fluctuates between 89.42 and 88.45%. For the rest of the study, the contact time is set at 30 minutes.

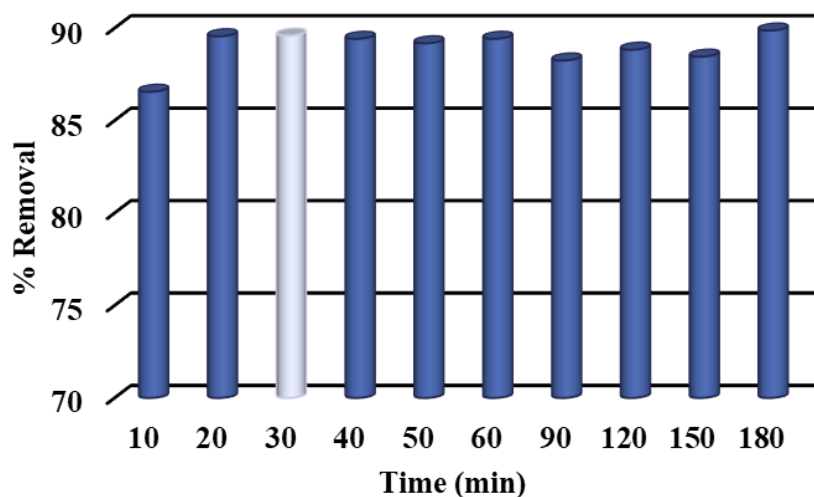


**Figure 2.** Effect of contact time on the adsorption capacity of DS.

The adsorbent dose is then studied (Figure 3). The mass of adsorbent is varied at constant volume (50 mL) from 0.1 g to 1g with a contact time of 30 minutes. The adsorption rate is 83.46% for an adsorbent mass of 0.1 g. It then decreases to 82.62% between 0.2 and 0.3 g. It then increases to finally reach a maximum value of 89.53% at 0.9 g before decreasing to 88.35% at 1 g. For the rest of the study, the contact time is set at 30 minutes and the mass of adsorbent is set at 0.9 g for 50 mL of solvent.

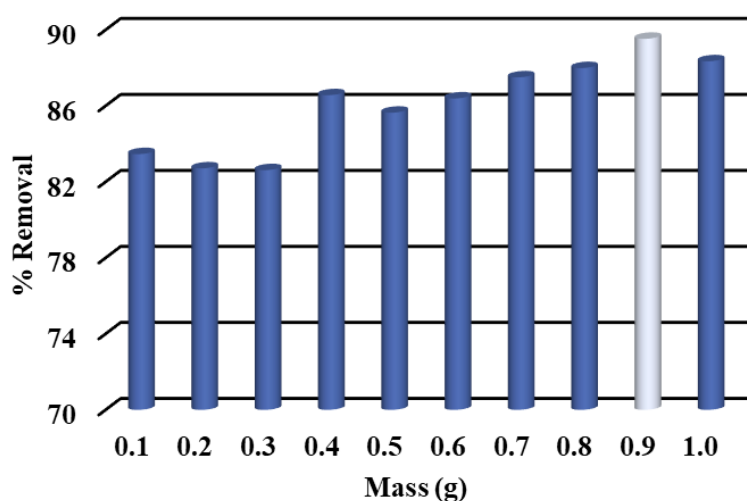


**Figure 3.** Effect of adsorbent dose on the removal capacity.

The influence of the particle size of the adsorbent on the adsorption rate is studied (Figure 4). A decrease in the adsorption rate is observed when the particle size increases. This phenomenon is probably due to the increase in specific surface area when the grain size decreases. For particle sizes between 1500 – 100  $\mu\text{m}$ , the adsorption rate varies between 74 %, and 86%. The maximum adsorption rate (90.7 %) is obtained for the particle size of 80  $\mu\text{m}$ .

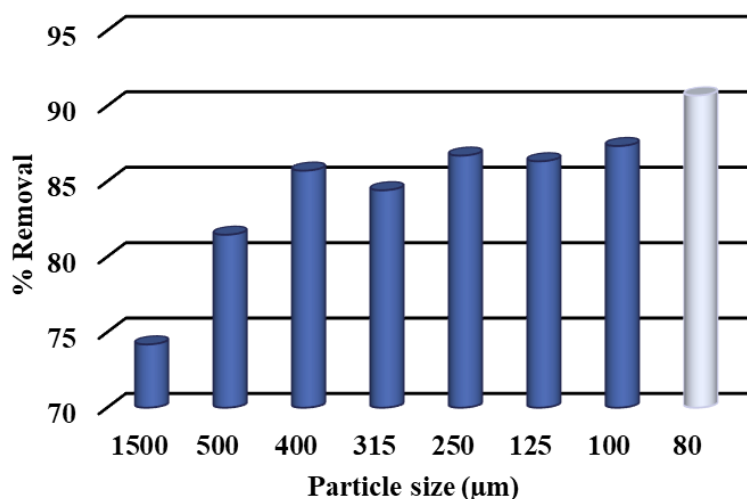


**Figure 4.** Effect of adsorbent particle size on the removal capacity.

The pH study is carried out for a particle size of 80 µm, a mass of 0.9 g for 50 mL of solvent, at 50 mg/L for methylene blue concentration and a contact time of 30 minutes (Figure 5). The pH of the zero charge point of the adsorbent is determined and is equal to 6.80. The zero charge point pH is the pH for which the charge on the adsorbent surface is zero. The influence of pH on the adsorption rate is significant because pH acts on the surface of the adsorbent and on the adsorbate. When the pH is higher than the zero charge point pH, the surface of the adsorbent is negatively charged, and the cations can easily interact with the surface of the adsorbent. When the pH is lower than the zero charge point pH, the surface of the adsorbent is positively charged, and the anions are well retained on the surface of the adsorbent. Since methylene blue is cationic, it interacts less well with the adsorbent surface when the latter has a positively charged surface. Indeed, competition with protons leads to a decrease in the number of sites available to fix methylene blue. Consequently, for strongly acidic pH, the adsorption rate is lower (79.22 %, pH = 2) and it increases when the pH increases to reach a maximum of 91.40 % for pH = 9. This is consistent with the increase in available binding sites at basic pHs.

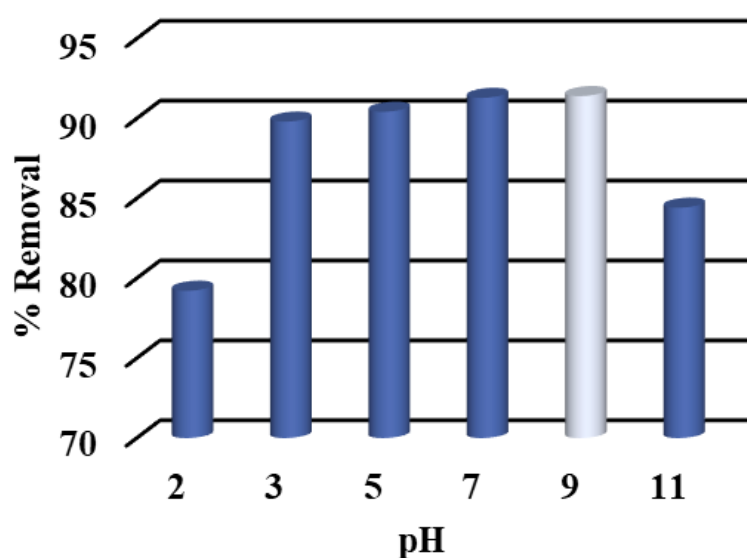


**Figure 5.** Effect of pH of the solution on the removal capacity.

The adsorption capacity is strongly linked to the initial concentration of the adsorbate in solution. In Figure 6, we note that the adsorption capacity reaches its maximum for a concentration of 50 ppm (92.72 %) and decreases slightly when the initial concentration of methylene blue varies from 60 ppm to 80 ppm before

increasing slightly between 80 and 100 ppm. It is observed that the adsorption rate increases from 88.88 % to 92.10 % between 10 and 40 ppm concentration.

Throughout the rest of the study, the following conditions are used: a dose of 0.9 g of adsorbent with particle size of 80  $\mu\text{m}$ , initial adsorbate concentration of 50 ppm and a contact time of 30 minutes at pH = 9.

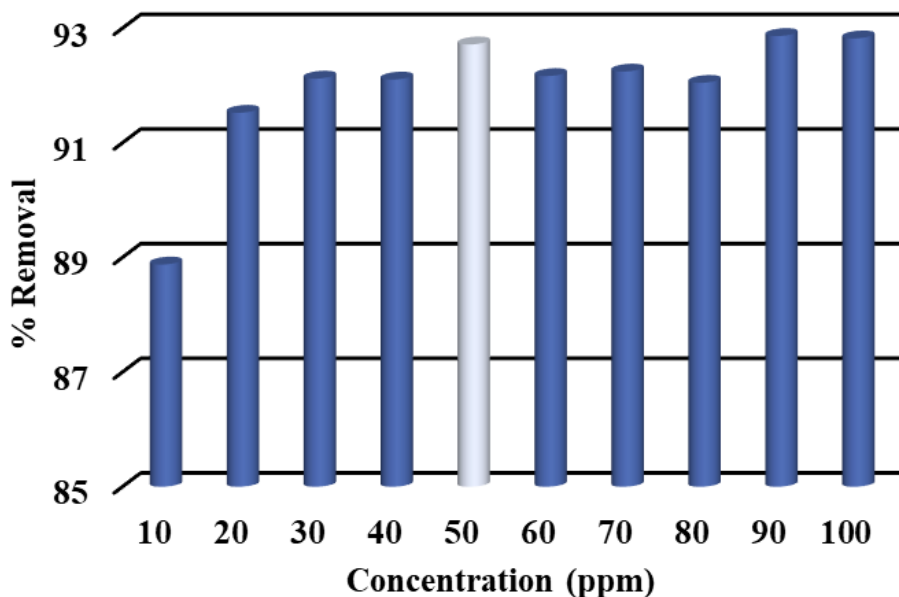


**Figure 6.** Effect of methylene blue initial concentration on the removal capacity.

### 3.3. Kinetic aspects

The kinetic studies of the adsorption of methylene blue on *Datura stramonium* leaf powder are carried out with a pH = 9, a temperature of 25°C, a concentration adsorbent of granulometry of 80  $\mu\text{m}$  of 18 g/L. Different initial concentrations of the adsorbate (10 to 100 ppm) are used. The aqueous concentrations of dyes were measured similarly, varying time contact. The amount of dye adsorbed  $q_t$  (mg/g) at time  $t$  is calculated using the following equation 1

$$\text{Equation 1: } q_t = \frac{(C_0 - C_t) \cdot V}{m_0}$$

where  $C_t$  (mg/L) is the aqueous dye concentration at time  $t$ ,  $C_0$  (mg/L) is the initial concentration of dye,  $V$  is the volume (L) and  $m_0$  (g) is the weight of adsorbent.

Four kinetic models: pseudo-first-order [26], pseudo-second-order [27], intra-particle diffusion model [28] and Elovich model [29] were examined in order to understand the adsorption mechanism on the leaves powder of *Datura stramonium*. The fit of these models was checked by each linear plot of the representative equation, respectively and by comparing to the regression coefficients for each expression. All the parameters of each model are presented in Table 1.

**Table 1.** Kinetic parameters of the adsorption on methylene blue.

$C_0$ (ppm)	$q_{e,exp}$ (mg/g)	Pseudo-first order			Pseudo-second order		
		$\ln(q_e - q_t) = \ln q_e - k_1 t$			$\frac{t}{q_t} = \frac{1}{k_2 q_e^2} + \frac{1}{q_e} t$		
		$k_1$ ( $\text{min}^{-1}$ )	$q_{e,cal}$ (mg/g)	$R^2$	$k_2$ (g/mg min)	$q_{e,cal}$ (mg/g)	$R^2$
10	0.506	-0.027	0.025	0.454	3.361	0.507	0.9997
20	1.027	-0.044	0.039	0.925	3.137	1.030	1.0000
30	1.556	-0.045	0.072	0.950	1.329	1.565	1.0000
40	2.056	-0.026	0.026	0.965	2.813	2.058	1.0000
50	2.600	-0.013	0.053	0.376	2.147	2.589	0.9999
60	3.078	-0.040	0.025	0.629	2.025	3.064	1.0000
70	3.596	-0.042	0.035	0.770	2.586	3.602	1.0000
80	4.127	-0.027	0.069	0.726	0.963	4.136	1.0000
90	4.656	-0.015	0.049	0.225	-13.330	4.630	1.0000
100	5.242	-0.024	0.185	0.433	0.304	5.269	0.9997
$C_0$ (ppm)	$q_{e,exp}$ (mg/g)	Intraparticle Diffusion			Elovich		
		$q_t = k_i t + I$			$q_t = \frac{1}{\beta} \ln \alpha \beta + \frac{1}{\beta} \ln t$		
		$k_i$ (mg/g min)	$I$	$R^2$	$\beta$ (g/mg)	$\alpha$ (mg/min)	$R^2$
10	0.506	0.006	0.461	0.635	61.728	$9.39 \times 10^9$	0.731
20	1.027	0.006	0.984	0.772	65.359	$3.70 \times 10^{25}$	0.855
30	1.556	0.009	1.487	0.978	45.455	$1.60 \times 10^{27}$	0.933
40	2.056	0.004	2.022	0.944	97.087	$5.91 \times 10^{82}$	0.904
50	2.600	0.010	2.511	0.573	35.714	$6.52 \times 10^{36}$	0.657
60	3.078	0.005	3.045	0.583	88.496	$4.56 \times 10^{114}$	0.489
70	3.596	0.007	3.547	0.767	54.348	$2.72 \times 10^{81}$	0.851
80	4.127	0.010	4.044	0.698	44.643	$2.21 \times 10^{76}$	0.582
90	4.656	0.006	4.595	0.161	52.356	$1.12 \times 10^{102}$	0.255
100	5.242	0.025	5.015	0.427	17.986	$3.58 \times 10^{37}$	0.321

### 3.3.1. Pseudo-first-order model

The Pseudo-first-order model proposed by Lagergren [26] is described by equation 2 which allows to estimate the performance of the adsorbent on the aqueous solution of the adsorbate. This model is based on the fact that the number of sites occupied by the adsorbates molecules is proportional to the number of free active sites.

$$\text{Equation 2: } \ln(q_e - q_t) = \ln q_e - k_1 t$$

where  $q_e$  is the equilibrium adsorption quantity (mg/g),  $q_t$  is the amount of dye adsorbed at time  $t$  (mg/g), and  $k_1$  is the rate constant ( $\text{min}^{-1}$ ). On plotting the Equation 2 (Figure 7), the parameters  $q_e$ , cal,  $k_1$  and  $R^2$  were calculated and reported in Table 1. The  $q_{e,cal}$  values do not fit the experimental  $q_{e,exp}$  values and the  $R^2$  values are very low. These facts are indicative of the pseudo-first-order model is not applicable to the process.

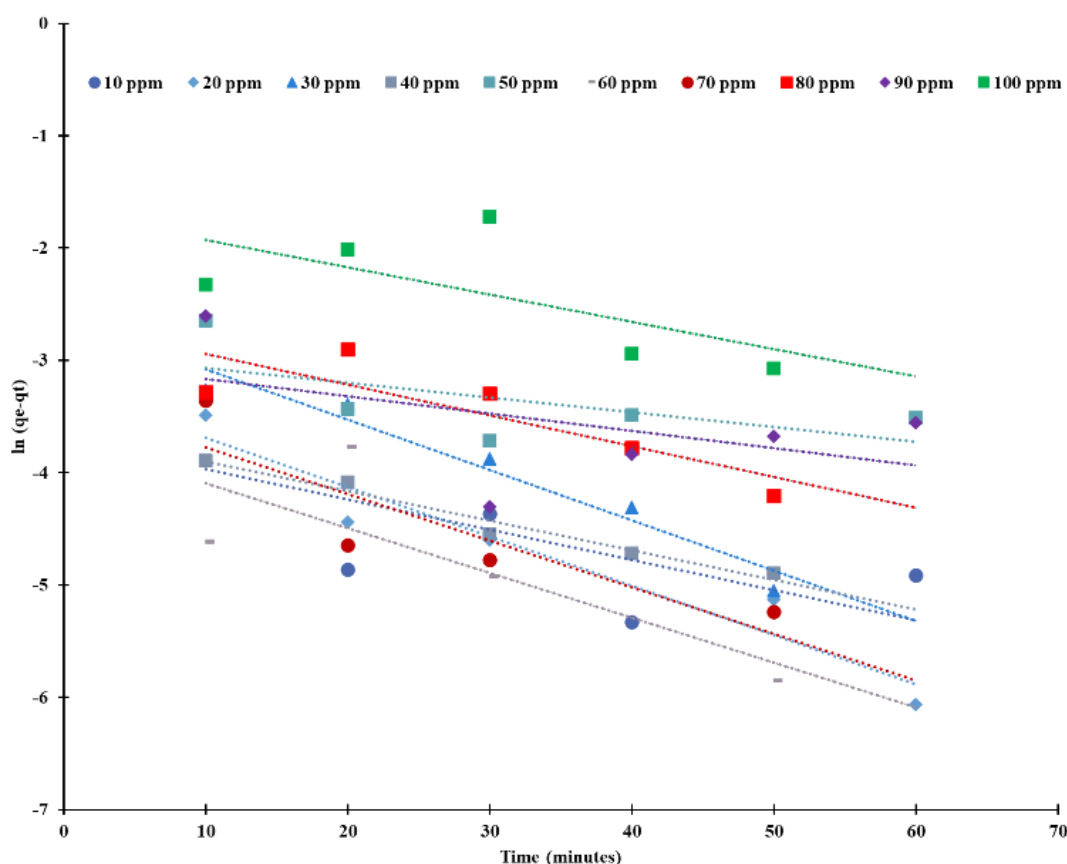


Figure7. Pseudo-first order Kinetic model for adsorption of methylene blue on DSL.

### 3.3.2. Pseudo-second-order model

The equation pseudo-second-order model is described by the equation 3 established by Ho and McKay's [27] assuming an interaction of two active sites with one unit of adsorbate. The linear form of this equation is given below:

$$\text{Equation 3: } \frac{t}{q_t} = \frac{1}{k_2 q_e^2} + \frac{t}{q_e}$$

where  $q_e$  is the equilibrium adsorption capacity (mg/g),  $q_t$ (mg/g) is the adsorption capacity at time  $t$ ,  $k_2$  (g/mg min) is the rate constant for the pseudo-first order kinetic model. On plotting the Equation 3 (Figure 8), straight

lines are observed for at different initial dyes concentrations (10 ppm to 100 ppm). The parameters  $q_{e,cal}$ ,  $k_2$  and  $R^2$  were calculated and reported in Table 1. The  $q_{e,cal}$  value fit the experimental  $q_{e,exp}$  value and the  $R^2$  value are close to the unit. These facts are indicative that the pseudo-second-order model is more suitable for the description of the adsorption process.

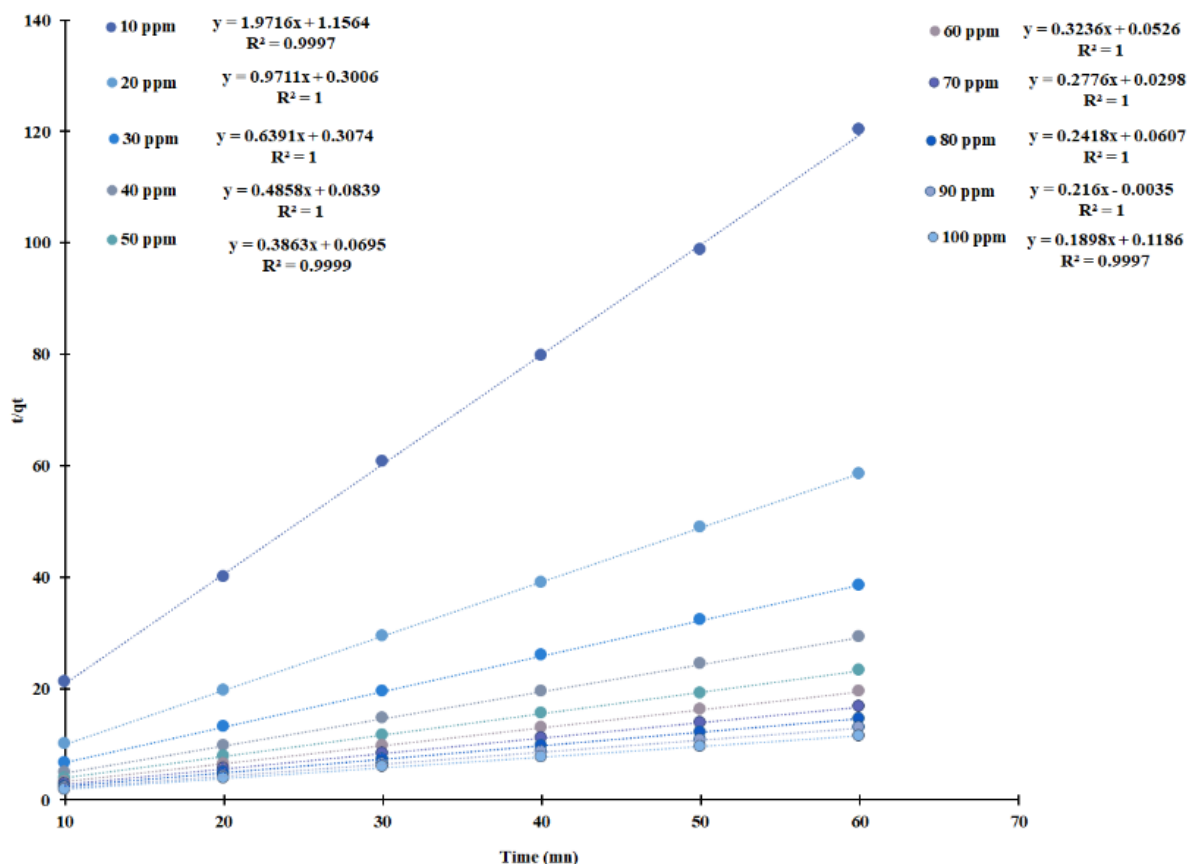


**Figure 8.** Pseudo-second order Kinetic model for adsorption of methylene blue on DSL.

### 3.3.3. Intra-particle diffusion model

The intra-particle diffusion model is described by the Equation 4 established by Weber and Morris [28].

$$\text{Equation 4: } q_t = k_i t^{1/2} + I$$

As reported in the literature [22] the plot of Equation 4 should be linear if intra-particle diffusion is involved in the adsorption mechanism. Additionally intra-particle diffusion is the rate-controlling step, if the straight line passes through the origin. If the straight line does not cross the origin, this is indicative that the intra-particle is not the only rate-controlling step. Figure 9 shows the plots of Equation 4 at different initial methylene blue concentrations (10 ppm to 100 ppm). All curves are not linear and do not pass through the origin and the correlation coefficients  $R^2$  very low. These observations are indicative that the intraparticle diffusion is not the rate-controlling step.

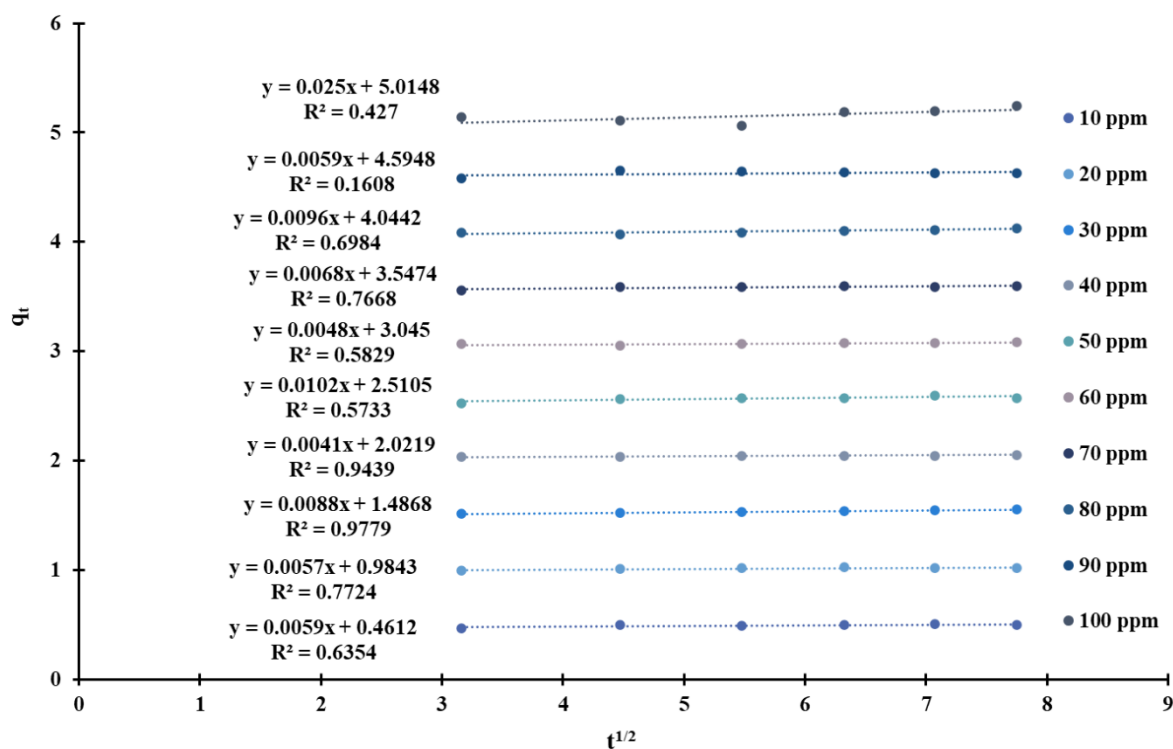


**Figure 9.** Intraparticle kinetic model for adsorption of methylene blue on DSL

### 3.3.4. Elovich model

The kinetic model called Elovich [29] is described by equation 5 which assumes the description of chemisorption on a heterogeneous surface.

$$\text{Equation 5: } q_t = \frac{1}{\beta} \ln(\alpha\beta) + \frac{1}{\beta} \ln t$$

where  $q_t$  is the amount of dye adsorbed (mg/g) at time (t),  $\alpha$  represents the initial sorption rate ( $\text{mg g}^{-1} \text{min}^{-1}$ ) and  $\alpha$  is related to the extent of surface coverage and activation energy for chemisorption ( $\text{g mg}^{-1}$ ). On plotting Equation 5 (Figure 10) no straight lines are observed for the different initial concentrations. The parameters  $\alpha, \beta$  and the correlation coefficients  $R^2$  are calculated from the plots and consigned in Table 1. The whole correlation coefficients were lower than the unit. This model is not suitable to study the sorption of methylene blue on leaves of *Datura stramonium*.

The sorption process of methylene blue on powder leaves of *Datura stramonium* is best described by the pseudo-second-order model as shown by the parameter's values consigned in Table 1.

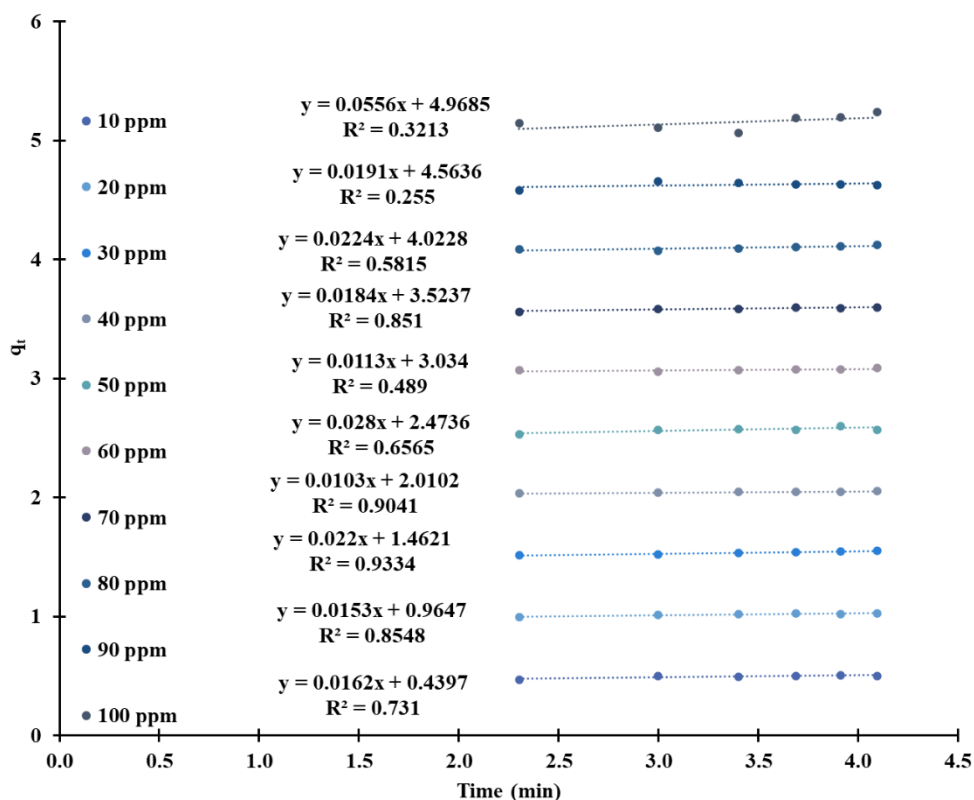


Figure 10. Elovich kinetic model for adsorption of methylene blue on DSL.

### 3.4. Isotherm

To understand how the adsorbed molecules are distributed between the liquid phase and the solid phase, which is constituted by the adsorbent, we study the relationship between the quantity of adsorbate adsorbed at equilibrium and the adsorbate concentration at equilibrium, which can be described by mathematical models called adsorption isotherm. The experimental data are analyzed by fitting them to different models. To find the best model for design purposes, isotherm model named Langmuir [30], Freundlich [31], Temkin [32], Dubinin-Radushkevich [33], Harkin-Jura [34] and Halsey [35] were used in this study.

#### 3.4.1. Langmuir isotherm

The Langmuir model assumes that the adsorbent has specific homogeneous active sites. This model suggests that when a site is occupied, there can be no further adsorption on that site. All sites are energetically equivalent and there is no interaction between molecules adsorbed on neighboring sites. This is a sorption monolayer on homogeneous active sites and can be expressed by equation 6.

$$\text{Equation 6: } \frac{C_e}{q_e} = \frac{1}{K_L Q_0} + \frac{C_e}{Q_0}$$

#### 3.4.2. Freundlich isotherm

On the other hand, in the Freundlich model, the adsorbent surface is assumed to be heterogeneous with a non-uniform distribution of the heat of adsorption over the surface. This model suggests multilayer sorption

with non-equivalent sites that are associated with adsorption energies resulting from the interaction between the adsorbed species.

$$\text{Equation 7: } \log q_e = \log K_F + \frac{1}{n} \log C_e$$

### 3.4.3. Temkin isotherm

The Temkin model is particularly used for the determination of the variation of the adsorption energy. It assumes that the decrease in the heat of sorption is linear. The Temkin isotherm can be expressed in the following linear form as in Equation 8.

$$\text{Equation 8: } \log q_e = B \log K_T + B \log C_e$$

### 3.4.4. Dubinin-Radushkevich isotherm

The Dubinin-Radushkevich model makes it possible to estimate the characteristic porosity of adsorbents and the apparent energy of adsorption. The linear form of the Dubinin-Radushkevich equation is reported as:

$$\text{Equation 9: } \ln q_e = \ln Q_{max} - B_D \varepsilon^2$$

where  $q_e$  is the adsorbed amount at equilibrium in mg/g,  $C_e$  is the equilibrium concentration in solution in mg/L,  $Q_{max}$  (mg/g) is the theoretical capacity of isotherm saturation and  $B_D$  ( $\text{mol}^2/\text{J}^2$ ) is the constant of the Dubinin-Radushkevich isotherm.  $\varepsilon = RT \ln \left( 1 + \frac{1}{C_e} \right)$ .

### 3.4.5. Harkin-Jura isotherm

The Harkin-Jura isotherm describes that the adsorbent has a heterogeneous pores distribution leading to multilayer adsorption of the adsorbate [36].

$$\text{Equation 10: } \frac{1}{q_e^2} = \frac{B_{HJ}}{A_{HJ}} - \frac{1}{A_{HJ}} \log C_e$$

### 3.4.6. Halsey isotherm

Hasley isotherm model developed by Hasley [35], describes floc formation at an equilibrium concentration. The Hasley adsorption equation is as shown in equation 11.

$$\text{Equation 11: } \ln q_e = \frac{1}{n_H} \ln K_H - \frac{1}{n_H} \ln C_e$$

Figure 11 shows the different linearized isotherm such as Langmuir, Freundlich, Temkin, Dubinin-Radushkevich, Harkin-Jura and Halsey for methylene blue. The estimated parameters ( $Q_0$ ,  $K_L$ ,  $\frac{1}{n}$ ,  $K_F$ ,  $B$ ,  $K_T$ ,  $Q_{max}$ ,  $B_D$ ,  $A_{HJ}$ ,  $B_{HJ}$ ,  $KH$  and  $1/n_H$ ) of all isotherms are summarized in Table 2. The values of the correlation coefficient  $R^2$ , which are important for estimating the fit quality are also reported in Table 2. The data in Table 2 show that methylene blue does not follow any of the studied models.

**Table 2.** Adsorption isotherms parameters.

Langmuir isotherm			Freundlich isotherm		
$\frac{C_e}{q_e} = \frac{1}{K_L Q_0} + \frac{1}{Q_0} C_e$			$\ln q_e = \ln K_F + \frac{1}{n} \ln C_e$		
$Q_0$ (mg/g)	$K_L$ (L/mg)	$R^2$	$\frac{1}{n}$	$K_F$	$R^2$
-22.124	-0.029	0.229	1.109	0.822	0.978
Temkin isotherm			Dubinin-Radushkevich		
$q_e = \frac{RT}{b_t} \ln K_T + \frac{RT}{b_t} \ln C_e$			$\ln q_e = \ln Q_{max} - B_D \varepsilon^2$		
$b_t$	$K_T$	$R^2$	$Q_{max}$	$B_D$	$R^2$
1103.807	1.100	0.881	4.596	$1 \times 10^{-6}$	0.893
Harkin-Jura			Halsey		
$\frac{1}{q_e^2} = \frac{B_{HJ}}{A_{HJ}} - \frac{1}{A_{HJ}} \log C_e$			$\ln q_e = \frac{1}{n_H} \ln K_H - \frac{1}{n_H} \ln C_e$		
$A_{HJ}$	$B_{HJ}$	$R^2$	$n_H$	$K_H$	$R^2$
0.292	0.683	0.674	-0.902	1.501	0.978

The Langmuir model is the least suitable for the experimental data of adsorption equilibrium data of adsorption equilibrium for methylene blue. The correlation coefficient  $R^2$  (0.229) is very low. It is also observed that the Temkin, Dubinin-Radushkevich and Harkin-Jura isotherms are not suitable to describe the adsorption of methylene blue by *Datura stramonium* leaf powder. The correlation coefficients  $R^2$  are, respectively, 0.881, 0.893 and 0.674 for the three isotherms. The experimental data of methylene blue adsorption were fitted by the Freundlich model with a fairly good correlation coefficient value of 0.978. Interactions between the adsorbed molecules occur, resulting in different energies of the adsorption reaction. The  $1/n$  value of 1.109 indicates a multimolecular adsorption mechanism. The  $K_F$  value of 0.822 indicates that the adsorption of methylene blue is not an easy task, compared to the results obtained with corn stalk tissue is used as adsorbent. In this case, the  $K_F$  varies in the range 10–320 depending on the pH of the solution [37]. The Halsey isotherm is also suitable to describe the adsorption of methylene blue on *Datura stramonium* leaf powder with a correlation coefficient  $R^2$  of 0.978.

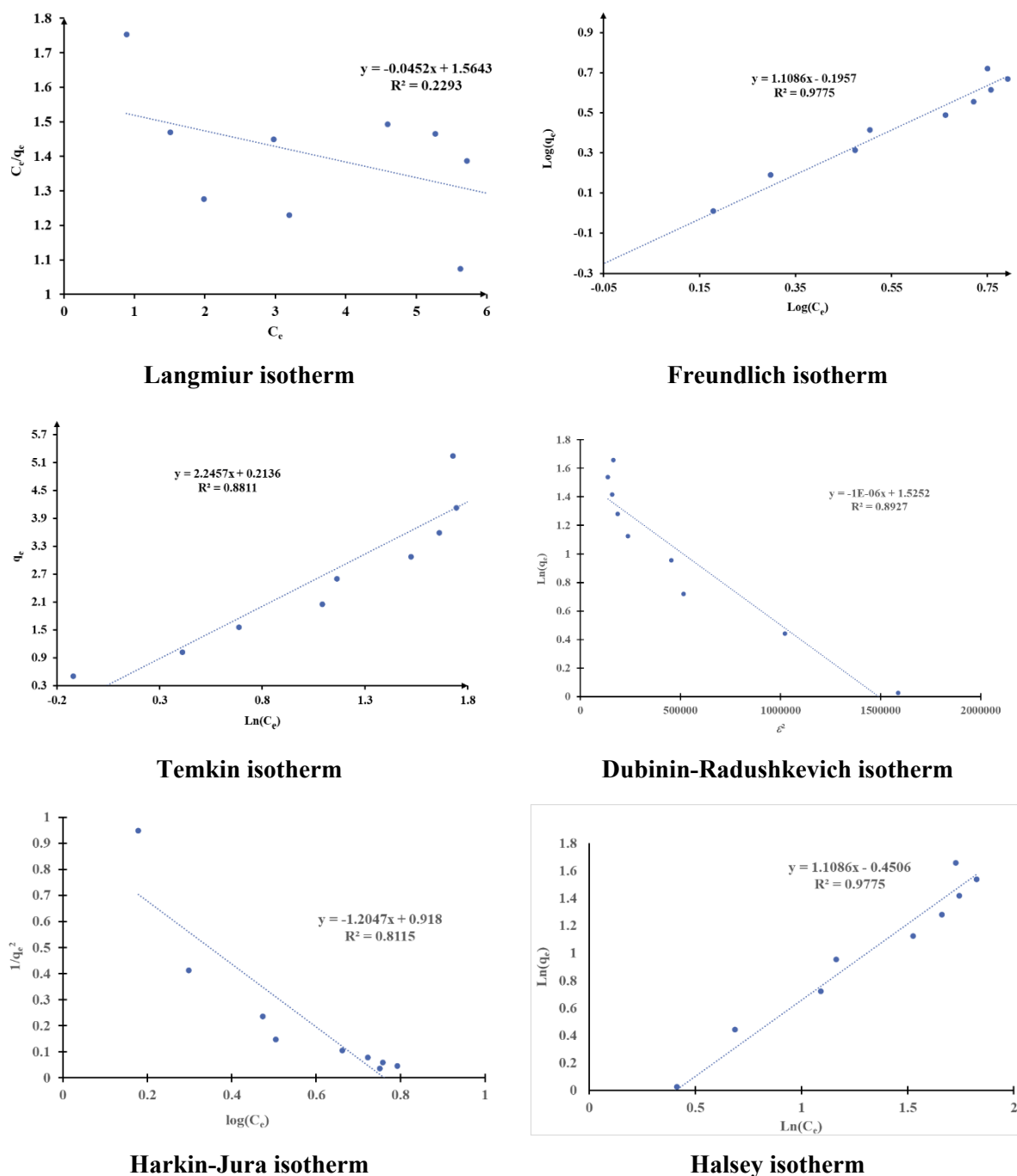


Figure 11. Different adsorption isotherms.

#### 4. Conclusion

The aim of the study was to determine the suitability of *Datura stramonium* adsorbent for the removal of methylene blue from aqueous solutions. The equilibrium agitation time for methylene blue sorption is 30 minutes. The optimum dosage for sorption is 18 g/L and the optimum size of adsorbent is 80  $\mu\text{m}$ . The optimal initial concentration of methylene blue is 50 ppm. Percentage sorption of methylene blue from the aqueous solution increases significantly with increase in pH from 2 (79.22 %) to 11 (84.42 %) with a maximum at pH 9 (91.40 %). The adsorption process is best described by the pseudo-second-order model. It is found that biosorption data are well represented by Freundlich ( $R^2 = 0.978$ ) and Halsey ( $R^2 = 0.978$ ) isotherms.

## References

- [1] Sharma, J., Sharma, S., & Soni, V. (2021). Classification and impact of synthetic textile dyes on Aquatic Flora: A review. *Regional Studies in Marine Science*, 45, 101802. <https://doi.org/10.1016/j.rsma.2021.101802>
- [2] Berradi, M., Hsissou, R., Khudhair, M., Assouag, M., Cherkaoui, O., Bachiri, A. E., & Harfi, A. E. (2019). Textile finishing dyes and their impact on aquatic environs. *Heliyon*, 5(11), e02711. <https://doi.org/10.1016/j.heliyon.2019.e02711>
- [3] Islam, T., Repon, Md. R., Islam, T., Sarwar, Z., & Rahman, M. M. (2023). Impact of textile dyes on health and ecosystem: a review of structure, causes, and potential solutions. *Environmental Science and Pollution Research*, 30(4), 9207-9242. <https://doi.org/10.1007/s11356-022-24398-3>
- [4] Sudarshan, S., Harikrishnan, S., Rathi Bhuvaneswari, G., Alamelu, V., Aanand, S., Rajasekar, A., & Govarthanam, M. (2022). Impact of textile dyes on human health and bioremediation of textile industry effluent using microorganisms: current status and future prospects. *Journal of Applied Microbiology*, 134(2), lxac064. <https://doi.org/10.1093/jambio/lxac064>
- [5] Kavil, Y. N., Shaban, Y. A., Alelyani, S. S., Al-Farawati, R., Orif, M. I., Ghandourah, M. A., Schmidt, M., Turki, A. J., & Zobidi, M. (2020). The removal of methylene blue as a remedy of dye-based marine pollution: a photocatalytic perspective. *Research on Chemical Intermediates*, 46(1), 755-768. <https://doi.org/10.1007/s11164-019-03988-w>
- [6] Wang, X., Zhi, L., & Müllen, K. (2008). Transparent, Conductive Graphene Electrodes for Dye-Sensitized Solar Cells. *Nano Letters*, 8(1), 323-327. <https://doi.org/10.1021/nl072838r>
- [7] Konstantinou, I. K., & Albanis, T. A. (2004). TiO<sub>2</sub>-assisted photocatalytic degradation of azo dyes in aqueous solution: kinetic and mechanistic investigations: A review. *Applied Catalysis B: Environmental*, 49(1), 1-14. <https://doi.org/10.1016/j.apcatb.2003.11.010>
- [8] Moorthy, A. K., Rathi, B. G., Shukla, S. P., Kumar, K., & Bharti, V. S. (2021). Acute toxicity of textile dye Methylene blue on growth and metabolism of selected freshwater microalgae. *Environmental Toxicology and Pharmacology*, 82, 103552. <https://doi.org/10.1016/j.etap.2020.103552>
- [9] Ramamurthy, K., Priya, P. S., Murugan, R., & Arockiaraj, J. (2024). Hues of risk: investigating genotoxicity and environmental impacts of azo textile dyes. *Environmental Science and Pollution Research*, 31(23), 33190-33211. <https://doi.org/10.1007/s11356-024-33444-1>
- [10] Dutta, S., Adhikary, S., Bhattacharya, S., Roy, D., Chatterjee, S., Chakraborty, A., Banerjee, D., Ganguly, A., Nanda, S., & Rajak, P. (2024). Contamination of textile dyes in aquatic environment: Adverse impacts on aquatic ecosystem and human health, and its management using bioremediation. *Journal of Environmental Management*, 353, 120103. <https://doi.org/10.1016/j.jenvman.2024.120103>
- [11] Al-Tohamy, R., Ali, S. S., Li, F., Okasha, K. M., Mahmoud, Y. A.-G., Elsamahy, T., Jiao, H., Fu, Y., & Sun, J. (2022). A critical review on the treatment of dye-containing wastewater: Ecotoxicological and health concerns of textile dyes and possible remediation approaches for environmental safety. *Ecotoxicology and Environmental Safety*, 231, 113160. <https://doi.org/10.1016/j.ecoenv.2021.113160>
- [12] Rovira, J., & Domingo, J. L. (2019). Human health risks due to exposure to inorganic and organic chemicals from textiles: A review. *Environmental Research*, 168, 62-69. <https://doi.org/10.1016/j.envres.2018.09.027>
- [13] Sanromán, M. A., Pazos, M., Ricart, M. T., & Cameselle, C. (2005). Decolourisation of textile indigo dye by DC electric current. *Engineering Geology*, 77(3), 253-261. <https://doi.org/10.1016/j.enggeo.2004.07.016>
- [14] Moyo, S., Makhanya, B. P., & Zwane, P. E. (2022). Use of bacterial isolates in the treatment of textile dye wastewater: A review. *Heliyon*, 8(6), e09632. <https://doi.org/10.1016/j.heliyon.2022.e09632>

- [15] Punzi, M., Anbalagan, A., Börner, R. A., Svensson, B.-M., Jonstrup, M., & Mattiasson, B. (2015). Degradation of a textile azo dye using biological treatment followed by photo-Fenton oxidation: Evaluation of toxicity and microbial community structure. *Chemical Engineering Journal*, 270, 290-299. <https://doi.org/10.1016/j.cej.2015.02.042>
- [16] Chollom, M. N., Rathilal, S., Alfa, D., & Pillay, V. L. (2015). The applicability of nanofiltration for the treatment and reuse of textile reactive dye effluent. *Water SA*, 41(3), 398-405. <https://doi.org/10.4314/wsa.v41i3.12>
- [17] Donkadokula, N. Y., Kola, A. K., Naz, I., & Saroj, D. (2020). A review on advanced physico-chemical and biological textile dye wastewater treatment techniques. *Reviews in Environmental Science and Bio/Technology*, 19(3), 543-560. <https://doi.org/10.1007/s11157-020-09543-z>
- [18] Mahjoub, B., Ncibi, M. C., & Seffen, M. (2008). Adsorption d'un colorant textile réactif sur un biosorbant non-conventionnel: Les fibres de *Posidonia oceanica* (L.) delile. *The Canadian Journal of Chemical Engineering*, 86(1), 23-29. <https://doi.org/10.1002/cjce.20005>
- [19] Aleem, M., Cao, J., Li, C., Rashid, H., Wu, Y., Nawaz, M. I., Abbas, M., & Akram, M. W. (2020). Coagulation- and Adsorption-Based Environmental Impact Assessment and Textile Effluent Treatment. *Water, Air, & Soil Pollution*, 231(2), 45. <https://doi.org/10.1007/s11270-020-4400-x>
- [20] Kallawar, G. A., & Bhanvase, B. A. (2024). A review on existing and emerging approaches for textile wastewater treatments: challenges and future perspectives. *Environmental Science and Pollution Research*, 31(2), 1748-1789. <https://doi.org/10.1007/s11356-023-31175-3>
- [21] Kumar, P. S., & Saravanan, A. (2017). 11 - Sustainable wastewater treatments in textile sector. In S. S. Muthu (Ed.), *Sustainable Fibres and Textiles* (pp. 323-346). Woodhead Publishing. <https://doi.org/10.1016/B978-0-08-102041-8.00011-1>
- [22] Gaye, A. A., Diouf, R., & Fall, A. (2023). Bio-sorption of methylene blue by defatted seed of *adansonia digitata*. *Earthline Journal of Chemical Sciences*, 9(1), 139-156. <https://doi.org/10.34198/ejcs.9123.139156>
- [23] Dior Samb, D., Gaye, A. A., & Fall, A. (2022). Bio-sorption of Methylene Blue by *Euphorbia hirta* leaves. *IOSR Journal of Environmental Science, Toxicology and Food Technology (IOSR-JESTFT)*, 16(6), 9-18. <https://doi.org/10.9790/2402-1606010918>
- [24] Gaye, A. A., & Nicolas Cyrille Ayessou, N. C. (2020). Bio-sorption of Methylene Blue and basic fuchsin from aqueous solution onto defatted *Carica papaya* seeds: mechanism and effect of operating parameters on the adsorption yield. *IOSR Journal of Environmental Science, Toxicology and Food Technology (IOSR-JESTFT)*, 14(2), 24-33. <https://doi.org/10.9790/2402-1402042433>
- [25] Akinyeye, O. J., Ibigbami, T. B., & Odeja, O. (2016). Effect of Chitosan powder prepared from Snail Shells to remove Lead (II) Ion and Nickel (II) Ion from aqueous solution and its adsorption isotherm model. *American Journal of Applied Chemistry*, 4(4), 146-156. <https://doi.org/10.11648/j.ajac.20160404.15>
- [26] Shahwan, T. (2015). Lagergren equation: Can maximum loading of sorption replace equilibrium loading? *Chemical Engineering Research and Design*, 96, 172-176. <https://doi.org/10.1016/j.cherd.2015.03.001>
- [27] Aichour, A., & Zaghouane-Boudiaf, H. (2019). Highly brilliant green removal from wastewater by mesoporous adsorbents: Kinetics, thermodynamics and equilibrium isotherm studies. *Microchemical Journal*, 146, 1255-1262. <https://doi.org/10.1016/j.microc.2019.02.040>
- [28] Weber, W. J., & Morris, J. C. (1963). Kinetics of adsorption on carbon from solution. *Journal of the Sanitary Engineering Division*, 89(2), 31-59. <https://doi.org/10.1061/JSEDAI.0000430>
- [29] Cope, F. W. (1972). Generalizations of the Roginsky-Zeldovich (or Elovich) equation for charge transport across biological surfaces. *The Bulletin of Mathematical Biophysics*, 34(3), 419-427. <https://doi.org/10.1007/BF02476452>

- [30] Marczewski, A. W. (2010). Analysis of kinetic Langmuir model. Part I: Integrated kinetic Langmuir equation (IKL): A new complete analytical solution of the Langmuir rate equation. *Langmuir*, 26(19), 15229-15238. <https://doi.org/10.1021/la1010049>
- [31] Debnath, S., & Das, R. (2023). Strong adsorption of CV dye by Ni ferrite nanoparticles for wastewater purification: Fits well the pseudo second order kinetic and Freundlich isotherm model. *Ceramics International*, 49(10), 16199-16215. <https://doi.org/10.1016/j.ceramint.2023.01.218>
- [32] Araújo, C. S. T., Almeida, I. L. S., Rezende, H. C., Marcionilio, S. M. L. O., Léon, J. J. L., & Matos, T. N. de. (2018). Elucidation of mechanism involved in adsorption of Pb(II) onto lobeira fruit (*Solanum lycocarpum*) using Langmuir, Freundlich and Temkin isotherms. *Microchemical Journal*, 137, 348-354. <https://doi.org/10.1016/j.microc.2017.11.009>
- [33] Ghezini, R., Sassi, M., & Bengueddach, A. (2008). Adsorption of carbon dioxide at high pressure over H-ZSM-5 type zeolite. Micropore volume determinations by using the Dubinin-Raduskevich equation and the “t-plot” method. *Microporous and Mesoporous Materials*, 113(1), 370-377. <https://doi.org/10.1016/j.micromeso.2007.11.034>
- [34] Erdogan, F. O. (2019). Freundlich, Langmuir, Temkin, DR and Harkins-Jura Isotherm studies on the adsorption of CO<sub>2</sub> on various porous adsorbents. *International Journal of Chemical Reactor Engineering*, 17(5), 20180134. <https://doi.org/10.1515/ijcre-2018-0134>
- [35] Halsey, G. D. (1952). The role of surface heterogeneity in adsorption. *Advances in Catalysis*, 4, 259-269. [https://doi.org/10.1016/S0360-0564\(08\)60616-1](https://doi.org/10.1016/S0360-0564(08)60616-1)
- [36] Ayawei, N., Ebelegi, A. N., & Wankasi, D. (2017). Modelling and interpretation of adsorption isotherms. *Journal of Chemistry*, 2017(1), 3039817. <https://doi.org/10.1155/2017/3039817>
- [37] Vučurović, V. M., Razmovski, R. N., Miljić, U. D., & Puškaš, V. S. (2014). Removal of cationic and anionic azo dyes from aqueous solutions by adsorption on maize stem tissue. *Journal of the Taiwan Institute of Chemical Engineers*, 45(4), 1700-1708. <https://doi.org/10.1016/j.jtice.2013.12.020>

---

This is an open access article distributed under the terms of the Creative Commons Attribution License (<http://creativecommons.org/licenses/by/4.0/>), which permits unrestricted, use, distribution and reproduction in any medium, or format for any purpose, even commercially provided the work is properly cited.

---